

Synthesis, Characterization and DFT Study of Pyrazole-Carboxamides Compounds

¹Abdullah Ghodran, Al-Sehemi*, ¹Ahmad Irfan**,

¹Yousry Ahmed Ammar and ¹Samir Bondock

¹Department of Chemistry, Faculty of Science, King Khalid University,
Abha 61413, P.O. Box 9004, Saudi Arabia.

²Unit of Science and technology, Faculty of Science, King Khalid University,
Abha 61413, P.O. Box 9004, Saudi Arabia.
agmasq@gmail.com*, irfaahmad@gmail.com**

(Received on 8th October 2012, accepted in revised form 20th May 2013)

Summary: We have synthesized pyrazole-carboxamides compounds; N [(1E)-(1,5-dimethyl-3-oxo-2-phenyl-2,3-dihydro-1H-pyrazol-4-yl) methylene]-2-(6-methoxy)-2-naphthyl)-propionyl hydrazide (4), N-[(1E)-(1,3-diphenyl-1H-pyrazol-4-yl)methylene]-2-(6-methoxy-2-naphthyl) propionyl hydrazide (5), 2-(6-Methoxy-naphthalen-2-yl)-1-(3-phenyl-pyrazol-1-yl)propan-1-one (6), 2-(6-Methoxy-naphthalen-2-yl) -1-(5-phenyl-2,3-dihydro-pyrazol-1-yl)propan-1-one (7) and 2-(6-methoxynaphthalen-2-yl)-N-{4-[3-(4-methoxyphenyl)-acryloyl]}-phenyl}-propionamide (8) then characterized by IR, ¹H-NMR and ¹³C-NMR techniques. Moreover two new hydrazide compounds have been designed. All the investigated compounds have been optimized by using density functional theory (DFT) at B3LYP/6-31G* level of theory. The electronic and charge transfer properties have been explained on the basis of highest occupied molecular orbitals (HOMOs), lowest unoccupied molecular orbitals (LUMOs) and density of states (DOS). The absorption spectra have been computed by using time dependent density functional theory (TDDFT) at TD-B3LYP/6-31G* level of theory. The 6 and 8 would be more stable due to less susceptible to oxidation with the significantly lowered LUMO energy levels. In 8, smaller HOMO-LUMO energy gap resulting red shift suggesting it would have better electron delocalization character than others.

Keywords: Ab initio calculations; Infrared spectroscopy; Nuclear magnetic resonance; Optical properties; Transport properties

Introduction

Long-term use of non-steroidal anti-inflammatory drugs (NSAIDs) like ibuprofen, naproxene, diclofenac, indomethacin and flurbiprofen have been associated with gastro-intestinal (GI) ulceration, bleeding and nephrotoxicity [1-3]. The pharmacological activity of NSAIDs is related to the suppression of prostaglandin biosynthesis from arachidonic acid by inhibiting cyclooxygenases [2, 4]. Chronic use of NSAIDs may elicit appreciable GI toxicity [5].

Therefore, by chemical modification NSAIDs have been synthesized previously. Studies described that the derivatization of the carboxylate resulted increased anti-inflammatory activity with reduced ulcerogenic effect [6-8]. Pyrazole derivatives have been reported to possess significant anti-inflammatory activity [9-14]. Syntheses of some potent analogues of naproxen have been found to possess an interesting profile of anti-inflammatory and analgesic activity with significant reduction in their ulcerogenic effect [14]. The major side effects of naproxen and their analogues are partly due to the corrosive nature of carboxylic acid group. In order to reduce or mask the side effects, some naproxen amide derivatives containing diaryl pyrazole moieties

were synthesized. We expect that the hydrolysis of these amides will produce the pyrazole and acid derivatives which affect in the same direction.

In the present study our aim is to synthesize drugs having interesting profile of anti-inflammatory activity with significant reduction of their ulcerogenic effect. We have replaced the carboxylic acid group of naproxene with additional heterocycles. The substitution pattern of the target compounds include various functionalities that would act as hydrogen-bond forming centers, such as the carbonyl, amide, amino, cyano, hydroxy and carbethoxy groups. Herein, we report the synthesis, characterization and density functional theory study of the new compounds N [(1E)-(1,5-dimethyl-3-oxo-2-phenyl-2,3-dihydro-1H-pyrazol-4-yl) methylene]-2-(6-methoxy)-2-naphthyl)-propionyl hydrazide, N-[(1E)-(1,3-diphenyl-1H-pyrazol-4-yl)methylene]-2-(6-methoxy-2-naphthyl)propionyl hydrazide, 2-(6-Methoxy-naphthalen-2-yl)-1-(3-phenyl-pyrazol-1-yl)propan-1-one, 2-(6-Methoxy-naphthalen-2-yl) -1-(5-phenyl-2,3-dihydro-pyrazol-1-yl)propan-1-one 2-(6-methoxynaphthalen-2-yl)-N-{4-[3-(4-methoxyphenyl)-acryloyl]}-phenyl}-propionamide, we also designed hydrazide derivatives; enol and keto

*To whom all correspondence should be addressed.

forms, see Fig. 1. We have investigated the electronic, photophysical and charge transfer properties. We investigated the N-N effect on the said properties. The effect of extended bridge on the electronic, photophysical and charge transfer properties has also been investigated.

Results and discussion

Electronic Properties

The distribution patterns of the frontier molecular orbitals; highest occupied molecular orbitals (HOMOs) and lowest unoccupied molecular orbitals (LUMOs) have been presented in Fig. 2. In **4**, most of the HOMO is delocalized between phenyl and naphthyl moieties. Phenyl has little contribution in the formation of HOMO. The LUMO is localized on the naphthyl moiety with contribution from keto oxygen and nitrogen atoms of pyrazol and hydrazide units. In **5**, HOMO is delocalized on whole of the compound and LUMO is also localized on most of the system with the exception of phenyl ring attached to carbon of pyrazol. In **6** and **7**, The HOMOs are

delocalized on 6-Methoxy-naphthalen moiety while LUMOs are localized on entire of the compounds. In **8**, the HOMO is delocalized on whole of the system while LUMO is localized on {4-[3-(4-methoxyphenyl)-acryloyl)]-phenyl}-propionamide side.

The comprehensible charge transfer has been observed in investigated compounds. In **4**, charge transferred from pyrazole and N-N moieties to naphthyl unit. In **5**, some charge transferred from pyrazole and phenyl units to naphthyl moiety. In **6** and **7**, charge transferred from naphthyl moiety to rest of the systems. In **8**, charge transferred from naphthyl moiety to central phenyl ring. In **9**, charge also transferred towards naphthyl moiety. Here we have observed that in **4**, **5**, **9**, and **10** compounds charge transferred toward naphthyl moieties while in **6-8** naphthyl moieties are behaving as donor groups. It is might be due to that the **4**, **5**, **9**, and **10** compounds have N-N azo group which favors to delocalize the charge on itself and its neighboring pyrazole. The trend in dipole moment has been observed as **4** > **6** > **9** > **8** > **10** > **5** > **7**.

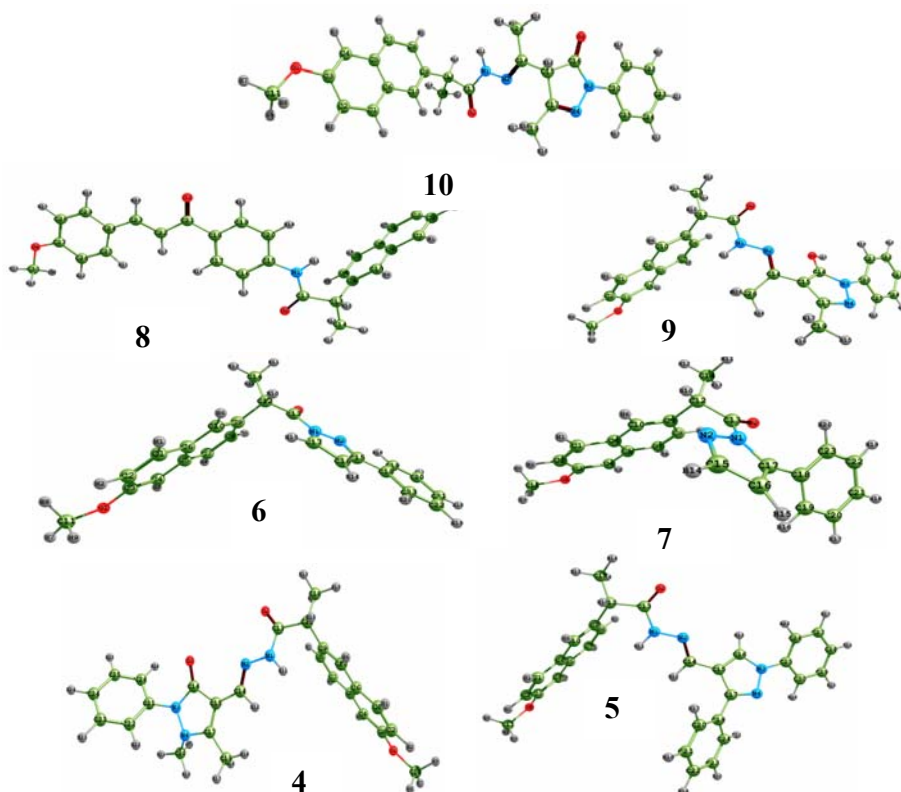


Fig. 1: Optimized geometries of the investigated compounds at DFT-B3LYP/6-31G* level of theory (C=green; N=blue; O=red; H=white).

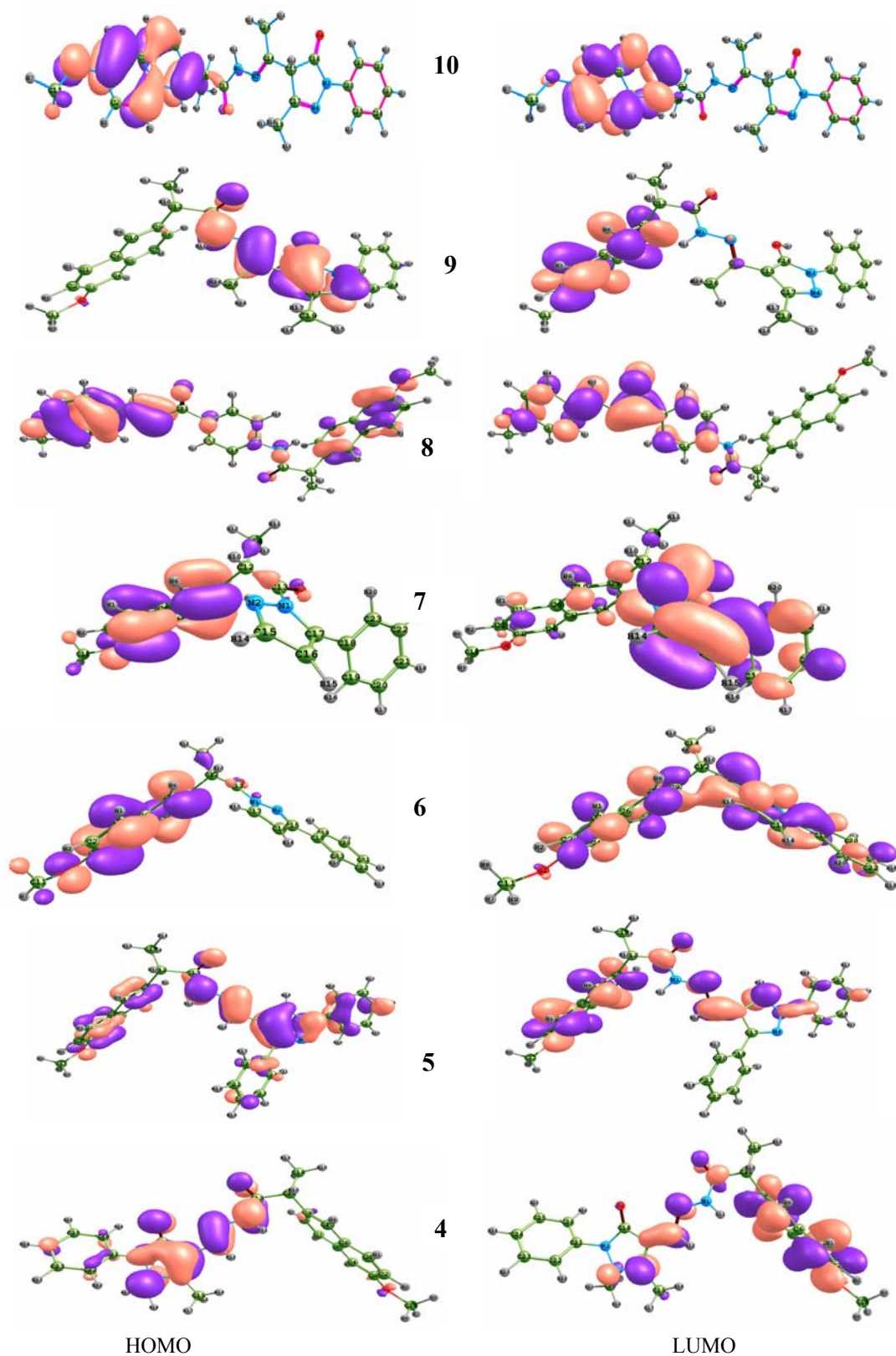


Fig. 2: The HOMO and LUMO distribution pattern of the investigated compounds.

The HOMO energies (E_{HOMO}), LUMO energies (E_{LUMO}) and HOMO-LUMO energy gap (E_{gap}) have been tabulated in Table 1. The trend of E_{HOMO} is as $7 = 9 > 4 > 10 > 5 > 6 > 8$. The tendency towards decreasing E_{LUMO} is $9 > 10 > 4 > 5 > 7 > 6 > 8$ and for E_{gap} $10 > 5 > 9 > 4 > 6 > 4b > 8$. It would be easy to excite the delocalized π -electrons having the smaller the E_{gap} resulting longer corresponding absorption wavelength [15]. The smallest E_{gap} has been observed for **8** while the largest for **10** followed by **5**. In conjugated systems the E_{gap} are governed by their chemical structures. The energy levels of HOMO and LUMO of **8** (-5.67 and -1.79 eV) are much lower than other investigated compounds. Long backbone of the π -conjugated system significantly lowers the energy level of the frontier molecular orbitals, see **8**. The considerably lowered E_{LUMO} level for **6** and **8** would be beneficent for the flow of electron and also makes these compounds less susceptible to oxidation revealing **6** and **8** would be more stable compounds. Similarly, **4**, **5** and **7** would be more stable than the **9** and **10** as E_{LUMO} of these compounds are lower than **9** and **10**.

Table-1: The HOMO Energy (E_{HOMO}), LUMO Energy (E_{LUMO}), HOMO-LUMO Energy Gap (E_{gap}) in eV and dipole moment (Debye) at B3LYP/6-31G* Level of Theory.

Molecules	E_{HOMO}	E_{LUMO}	E_{gap}	Dipole moments
4	-5.44	-1.21	4.23	10.02
5	-5.56	-1.24	4.32	3.82
6	-5.63	-1.41	4.21	4.88
7	-5.37	-1.37	4.00	2.83
8	-5.67	-1.79	3.88	4.53
9	-5.37	-1.13	4.24	4.85
10	-5.54	-1.14	4.40	4.51

Density of States

Fig. 3 illustrates the density of state (DOS) which plays an important role in various physical systems where HOMO and LUMO are shown by green and blue lines, respectively and region between green and blue lines represents the energy gap.

The E_{HOMO} and E_{LUMO} are -5.44 eV and -1.21 eV, respectively shows the E_{gap} 4.23 eV in **4**. In **5**, the E_{HOMO} and E_{LUMO} are -5.56 eV and -1.24 eV, respectively. In **6/7** HOMO and LUMO have energies -5.63 eV/-5.37 eV and -1.41 eV/-1.37 eV, respectively. In **8**, HOMO and LUMO have -5.67 eV and -1.79 eV energies, respectively. The E_{HOMO} and E_{LUMO} are -5.37 eV (-5.54 eV) and -1.13 eV (-1.14 eV) in **9** (**10**), respectively. The availability of states in HOMO is higher than LUMO in **4**, **5**, **8**, **9**, and **10**. In **6** and **7**, the states in HOMO and LUMO is almost identical. In most of the cases the energy difference between different HOMOs (HOMO, HOMO1,

HOMO2, HOMO3 etc.) is smaller than the LUMOs (LUMO, LUMO1, LUMO2, LUMO3 etc.), Fig. 3.

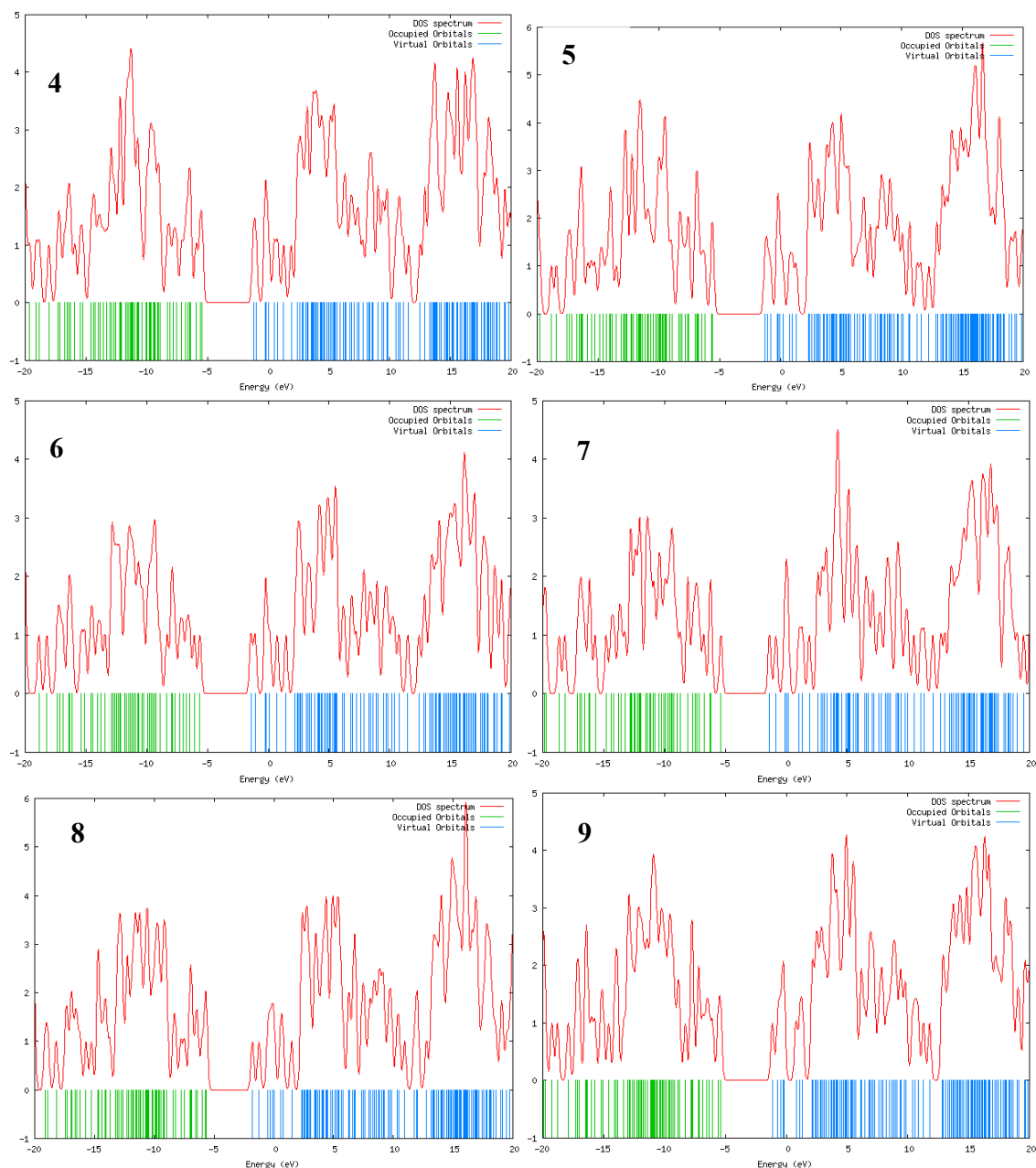
Photophysical Properties

Fig. 4 illustrates the absorption wavelengths (nm) and oscillator strengths (f) of the studied compounds computed at the TD-B3LYP/6-31G* level of theory. The **4** has two absorption spectrum peaks; maximum one is broaden from 309-326 nm while second peak observed at 287 nm. The maximum absorption peak has been observed at 312 nm in **5**. The maximum absorption peaks in **6** and **7** have been observed at 291 and 297 nm, respectively. Two more absorption peaks (at 247 nm, and 331 nm) and one shoulder peak at 269 nm have also been viewed in **6**. Similarly, three more peaks have been observed in **7** at 249, 267 and 355 nm. The maximum absorption peak in **8** has been observed at 351 nm. In **9** two absorption peaks have been observed at 267 nm (maximum absorption peak) and 296 nm. In **10**, maximum absorption peak can be seen at 293 nm. The smallest HOMO-LUMO energy gap has been observed for **8** resulting red shifted compared to all other studied compounds (31-84 nm compared to other compounds) suggesting that it would have better electron delocalization character than others. In general, larger oscillator strengths correspond to larger experimental absorption coefficients [15]. It can be seen that **8** has larger oscillator strength compared other studied compounds revealing it would have larger absorption coefficient.

We have studied the nine electronic transition states, see supporting information for detail. In **4**, S_0 - S_1 state remains dominated with maximum absorption and this state is caused by H \rightarrow L with 95% contribution. The second state caused by H-1 \rightarrow L with 90% contribution. The third state has 81% contribution transition from H \rightarrow L+1 and the fourth state is derived from H-1 \rightarrow L+1 with 89% contribution while all other states have less than 50% contribution of different frontier molecular orbitals. In **5**, the main transitions are as follows: H \rightarrow L (94%), H-1 \rightarrow L (91%), H \rightarrow L+1 (91%), H-1 \rightarrow L+1 (86%), H \rightarrow L+2 (83%), H-2 \rightarrow L (76%) for first, second, third, fourth, fifth and eighth states, respectively. In **6**, S_0 - S_1 is dominant with the H \rightarrow L transition having 96% contribution. The second, third, fourth, fifth, sixth, seventh, and ninth states are derived from H \rightarrow L+1, H-1 \rightarrow L, H-2 \rightarrow L, H-6 \rightarrow L, and H-5 \rightarrow L, H-1 \rightarrow L+1, H-3 \rightarrow L, and H-4 \rightarrow L, with 81%, 95%, 51%, 50%, 87%, 76% and 89% contribution, respectively. In **7**, S_0 - S_1 transition is caused by H \rightarrow L with 97% contribution. Transition

of second state is dominated with 95% contribution from H-1 \rightarrow L. The second, sixth, eighth, and ninth states are derived from H \rightarrow L+1, H-3 \rightarrow L, H \rightarrow L+2, and H-2 \rightarrow L+1, and H-5 \rightarrow L, H-1 \rightarrow L+1, H-3 \rightarrow L, and H-4 \rightarrow L, with 74%, 63%, 52%, and 83%, contribution, respectively. The main transition in **8** is also from H \rightarrow L (89%) which is second state. The first, third, fourth, fifth, sixth, seventh, eighth and ninth states have major transitions from H-3 \rightarrow L, H-1 \rightarrow L, H-2 \rightarrow L, H-1 \rightarrow L+1, H \rightarrow L+1, H-2 \rightarrow L+1, H-4 \rightarrow L and H-5 \rightarrow L with the contribution 94%, 95%,

83%, 55%, 52%, 79%, 74% and 83%, respectively. In **9**, S₀-S₁ state remains dominated with maximum absorption and this state is caused by H \rightarrow L with 98% contribution. The second, third, fourth, seventh, eighth and ninth states have 88, 96, 97, 90, 77, and 83% contribution from H-1 \rightarrow L, H \rightarrow L+1, H \rightarrow L+2, H-2 \rightarrow L, H \rightarrow L+3, and H \rightarrow L+4 excitations, respectively. In **10** only first and second states have more than 50% contribution, i.e., H \rightarrow L (86%) for first state and H \rightarrow L+1 (54%) for second state.



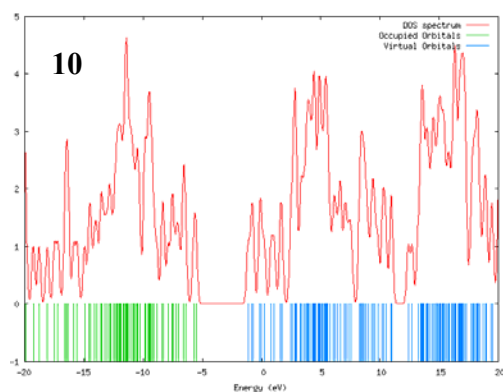


Fig. 3: Density of states of the investigated systems at B3LYP/6-31G* level of Theory.

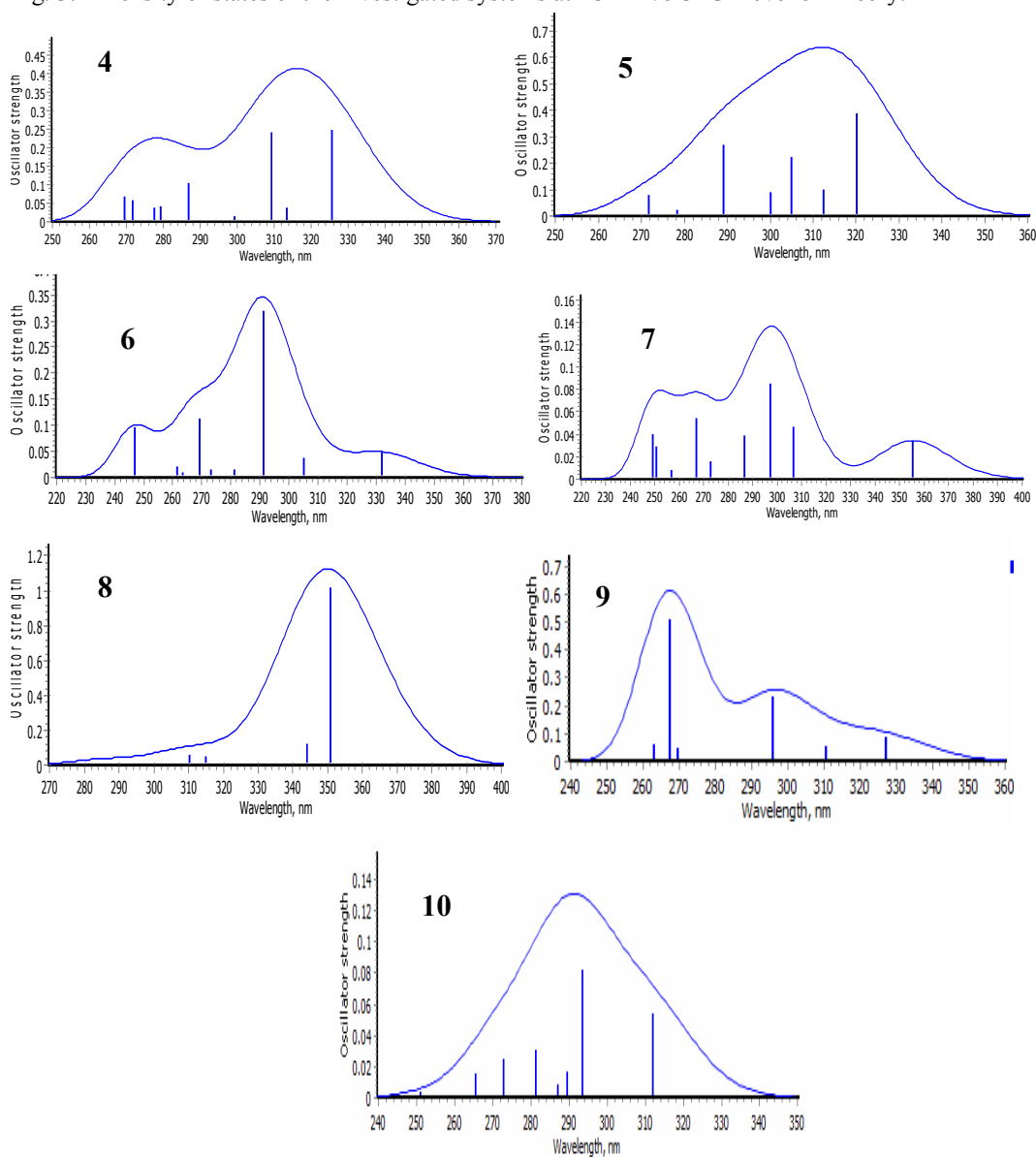


Fig. 4: The absorption spectra of the investigated compounds at TD-B3LYP/6-31G* level of Theory.

Experimental

The starting material 2-(6-methoxy-2-naphthyl)propanoic acid hydrazide (**3**) was prepared by esterification of 2-(6-methoxy-2-naphthyl)propanoic acid (**1**) (see supporting informations) followed by treatment with hydrazine hydrate in absolute ethanol [14]. The structures of the ester and hydrazide derivatives were confirmed through $^1\text{H-NMR}$ and $^{13}\text{C-NMR}$. The hydrazide derivatives have proven to be a good synthons for different highly biological active heterocyclic compounds. In fact, some evidences suggest that the hydrazone moiety possess a pharmacophoric character for the inhibition of COX [16-18]. Thus, we decided to replace the carboxylic acid moiety of naproxene with an N-arylhydrazone group. The condensation of the hydrazide derivative **3** with pyrazolo carbonyl compounds in ethanol at reflux condition furnished the corresponding hydrazono derivatives (**4** and **5**).

2-(6-Methoxy-2-naphthyl)propanoic acid hydrazones (**4**) and (**5**)

To a solution of the hydrazide derivative **3** (0.01 mol) in ethanol (30 mL), 1,5-dimethyl-3-oxo-2-phenyl-3-dihydro-1H-pyrazol-4-carboxaldehyde or 1,3-phenyl-1H-pyrazole-4-carboxaldehyde (0.01 mol) was added. The reaction mixture was refluxed for 3h, the obtained product was crystallized from the proper solvent (Details can be found in supporting information).

N [(1E)-(1,5-dimethyl-3-oxo-2-phenyl-2,3-dihydro-1H-pyrazol-4-yl) methylene]-2-(6-methoxy-2-naphthyl)-propionyl hydrazide (**4**): yield (74%) crystallized from ethanol, m.p. 213-215 °C, $\text{C}_{26}\text{H}_{26}\text{N}_4\text{O}_3$ (442.51): C, 70.57; H, 5.92; N, 12.60. Found: C, 70.43; H, 5.84; N, 12.71%. IR: 3352 (NH), 2969, 2935(CH-SP3), 1670, 1656(2C=O), 1604 (C=N). $^1\text{H-NMR}$ (DMSO- d_6): 1.43(d, $J=6.5\text{Hz}$, 3H, CH_3), 2.56 (s, 3H, CH_3), 3.22 (s, 3H, N- CH_3), 3.62 (q, $J=6.5\text{Hz}$, 1H, CH), 3.86 (s, 3H, OCH_3), 7.12-7.81 (m, 11H, Ar-H), 8.01 (s, 1H, N=CH), 10.99 (bs, 1H, NH). $^{13}\text{C-NMR}$: 12.12(CH_3), 18.74 (CH_3), 40.1(CH), 45.9 (N- CH_3), 55.1 (OCH_3), 105.6 (C-5), 118.3(C-7), 124.1(C-4), 125.5(C-8a), 126.31, 127.5, 128.4, 129.3, 130.3, 132.9, 133.9, 135.6, 136.5, 137.4, 137.7, 139.0, 141.9, 145.3, 156.7, 171.9, 176.7.

N-(1E)-(1,3-diphenyl-1H-pyrazol-4-yl)methylene]-2-(6-methoxy-2-naphthyl) propionyl hydrazide (**5**): yield (65%), crystallized from ethanol, m.p. 195-196 °C, Anal. Calcd for $\text{C}_{26}\text{H}_{13}\text{N}_4\text{O}_2$

(474.55): C, 75.93; H, 5.52; N, 11.81. Found: C, 75.85; H, 5.64; N, 11.76%. IR: 3191(NH), 3052(CH-Ar), 2969-2934 (CH-sp3), 1655(C=O), 1602(C=N). $^1\text{H-NMR}$ (DMSO- d_6): 1.48(d, $J=6.5\text{Hz}$, 3H, CH_3), 3.84 (s, 3H, OCH_3), 4.1(q, $J=6.5\text{Hz}$, 1H, CH), 7.24-8.77(m, 16H, Ar-H), 8.29 (s, 1H, Pyrazol- H_5), 8.95(s, 1H, CH=N), 11.12(bs, 1H, NH). $^{13}\text{C-NMR}$ 18.2(CH_3), 43.94 (CH), 55.9 (OCH_3), 105.6, 116.6, 116.9, 118.6, 118.7, 125.3, 125.7, 126.2, 126.9, 127.6, 128.3, 128.6, 128.9, 129.5, 131.9, 132.3, 133.2, 135.5, 136.4, 136.9, 138.9, 139.5, 151.7, 151.1, 156.8, 156.9, 169.3, 174.6.

2-(6-Methoxy-naphthalen-2-yl)-1-(3-phenyl-pyrazol-1-yl)propan-1-one (**6**): The hydrazide derivative **3** was used as binucleophile for the synthesis of pyrazole derivatives. Thus, treatment of the hydrazide **3** with 3-dimethylamino-1-phenyl-propenone or 3-dimethylamino-1-thiophen-2-ylpropenone as enaminone in acetic acid under reflux caused cyclization to afford the pyrazole derivatives **6**. The products were formed via initial addition of the amino group in hydrazine to the enaminone double bond, followed by elimination of dimethylamine.

To a solution of the enaminone derivatives (0.01 mol) in acetic acid (12 mL), the hydrazide derivative **3** (0.01 mol) was added the mixture was heated under reflux for 8 h. The reaction mixture was treated with ice and the formed product was filtered and crystallized from ethanol. Yield (76%), m.p. 187-188 °C; Anal. Calcd for $\text{C}_{23}\text{H}_{20}\text{N}_2\text{O}_2$ (356.42): C, 77.71; H, 5.66; N, 7.86. Found: C, 77.62; H, 6.58; N, 7.75.

The structure of **6** was substantiated by the $^1\text{H-NMR}$ spectra which displayed new pair of doublets at δ 7.12 and 7.77 ppm with ($J = 7.5\text{Hz}$) corresponding to pyrazole protons at positions 4 and 5, respectively.

IR (KBr); 3065(CH-Ar), 2978-2942 (CH-sp3), 1667(C=O), 1597(C=N); $^1\text{H NMR}$ (DMSO- d_6) δ = 1.43 (d, $J=6.5\text{Hz}$, 3H, CH_3), 3.77 (q, $J=6.5\text{Hz}$, 1H, CH), 3.86 (s, 3H, OCH_3), δ 7.12 -7.77 (2d, $J=7.5\text{Hz}$, 2H, H_4 , H_5 -pyrazole), 7.14-7.76 (m, 11H, Ar-H). $^{13}\text{C-NMR}$ 18.12, (CH_3), 42.71 (CH), 55.02 (OCH_3), 105.55, 118.36, 125.01, 125.29, 125.92, 126.36, 126.47, 126.65, 127.30, 127.79, 128.21, 128.57, 128.92, 129.94, 133.09, 136.48, 136.51, 156.91, 172.12, 172.28.

2-(6-Methoxy-naphthalen-2-yl)-1-(5-phenyl-2,3-dihydro-pyrazol-1-yl)propan-1-one (**7**): The reaction of compound **3** with 3-dimethylamino-

1-phenylpropan-1-one hydrochloride in ethanol containing acetic acid affected cyclization to give 2-(6-methoxynaphthalen-2-yl)-1-(5-phenyl-2,3-dihydro-pyrazol-1-yl)propan-1-one (**7**).

A mixture of the hydrazide **3** (0.01 mol) and 3-dimethyl amino-1-phenyl-propan-1-one hydrochloride (0.01mol) in ethanol 20mL containing 5 mL of acetic acid was refluxed for 8 h. The reaction mixture was cooled and treated with ice and the formed product was filtered and crystallized from ethanol. Yield (76%), m.p. 254-255 °C; Anal. Calcd for $C_{23}H_{22}N_2O_2$ (358.43): C, 77.07; H, 6.19; N, 7.82. Found: C, 77.60; H, 6.34; N, 7.72. IR (KBr); 3128(NH), 3035(CH-Ar), 2974-2946 (CH-sp³), 1663(C=O), 1611(C=N); ¹H-NMR (DMSO-d₆) δ = 1.44 (d, J=6.5 Hz, 3H, CH₃), 1.94 (s, 2H, CH₂-pyrazoline), 3.83 (q, J=6.5Hz, 1H, CH), 3.86 (s, 3H, OCH₃), 4.8(s, 1H, CH-pyrazoline), 7.12 -7.79 (m, 11H, Ar-H), 8.9 (s, 1H, NH). ¹³C-NMR 18.04, (CH₃), 35.80, 42.71 (CH), 55.02 (OCH₃), 60.22, 105.66, 118.57, 125.53, 126.14, 126.66, 127.59, 127.93, 128.11, 128.32, 128.53, 128.62, 128.66, 129.12, 132.97, 136.45, 137.26, 156.80, 172.30.

2-(6-methoxynaphthalen-2-yl)-N-{4-[3-(4-methoxyphenyl)-acryloyl]-phenyl}-propionamide (**8**): The propen-1-one derivative (**8**) was prepared by the reaction of acetyl derivative with appropriately substituted aldehydes in ethanol medium employing alcoholic sodium hydroxide as the catalyst at 0-5 °C. Equimolar quantities of the requisite aldehyde (0.01 mol) and N-(4-acetylphenyl)-2-(6-methoxynaphthalen-2-yl)propanamide (0.01 mol) were dissolved in minimum amount of alcohol. Sodium hydroxide solution (0.02 mol) was added slowly and the mixture stirred for 2h until the entire mixture becomes very cloudy. Then the mixture was poured slowly into 400 ml of water with constant stirring and kept in refrigerator for 24 hours. The precipitate obtained was filtered, washed and recrystallized from ethanol.

Yield (77%), m.p. 229-231°C, Calc. for $C_{30}H_{27}NO_4$ (465.54): C, 77.40; H, 5.85; N, 3.01. Found: C, 77.65; H, 5.68; N, 3.27. IR: ν_{max} /cm⁻¹ 3244 (NH), 2975, 2839 (CH-aliph), 1659 (C=O). ¹H-NMR (DMSO-d₆): δ = 1.52 (d, J=6.5 Hz, 3H, CH₃), 3.82, 3.86 (2s, 6H, 2OCH₃), 3.87 (q, 1H, CH), 7.01-8.14 (m, 16H, Ar-H+CH=CH), 10.53 (s, 1H, NH). ¹³C-NMR: 18.40 (CH₃), 44.35 (CH), 55.06, 55.59 (2OCH₃), 105.61, 114.29, 118.44, 118.63, 119.32, 125.14, 126.20, 126.80, 127.33, 128.30, 129.07, 129.62, 130.60, 131.72, 132.42, 133.20, 136.56,

143.26, 143.43, 157.03, 161.17, 164.13, and 172.88, 187.27 (2C=O).

Computational Details

All the calculations have been performed by using Gaussian09 package [19]. The ground state geometries have been optimized using density functional theory (DFT) [20-34] with B3LYP [33-37] and 6-31G* basis set [38] which have been proved an efficient approach. The frequencies have also been computed at the same level of theory and no imaginary frequencies have been observed. The absorption spectra have been computed by using time dependent density functional theory (TDDFT) [39, 40] at TD-B3LYP/6-31G* level of theory. The DOS and UV-Visible Spectrum of these systems were convoluted using GaussSum 2.1 software [41].

Conclusions

The pyrazole-carboxamides anti-inflammatory drugs were successfully synthesized and characterized by IR, ¹H-NMR and ¹³C-NMR techniques. Ground state geometries, electronic and charge transfer properties were computed by DFT. The absorption spectra were calculated by TDDFT. The comprehensible intra-molecular charge transfer has been observed in investigated drugs. In **4**, **5**, **9** and **10** drugs charge transferred towards naphthyl moieties while in **6-8** naphthyl moieties are behaving as donor groups. The π -conjugated long backbone of **8** significantly lowers the energy level of the HOMO and LUMO. The lowered LUMO energy level for **6** and **8** would favor the flow of electron and makes these compounds less susceptible to oxidation. The better electron delocalization character has been observed in **8**. The maximum absorption wavelength of **8** is red shifted compared to all other studied drugs. The S₀-S₁ state remains dominated with maximum absorption which is caused by H \rightarrow L.

Supporting Information

Schematic diagrams of investigated compounds, computed transition and their assignments, contribution, oscillator strengths, IR, and NMR spectra can be found in supporting information.

Acknowledgement

The authors are thankful to the Deanship of the Scientific Research King Khalid University for funding through the project KCU.

References

1. M. B. Kimmey, *Journal of Rheumatology*, **19**, 68 (1992).
2. C. J. Smith, Y. Zhang, C. M. Koboldt, J. Muhammad, B. S. Zwefel, A. Shaffer, J. J. Talley, J. L. Masferrer, K. Serbert and P. C. Isakson, *Proceedings of the National Academy of Sciences*, **95**, 13313 (1998).
3. C. Hawkey, L. Laine, T. Simon, A. Beaulieu, J. Maldonado-Cocco, E. Acevedo, A. Shahane, H. Quan, J. Bolognese and E. Mortensen, *Arthritis Rheumat*, **43**, 370 (2000).
4. T. D. Warner, F. Giuliano, I. Vaynovie, A. Bukasa, J. A. Mitchell and J. R. Vave, *Proceedings of the National Academy of Sciences*, **96**, 7563 (1999).
5. F. L. Lanza, *the American Journal of Gastroenterology*, **93**, 2037 (1998).
6. A. S. Kalgutkar, A. B. Marnett, B. C. Crews, R. P. Remmel and L. J. Marnett, *Journal of Medicinal Chemistry*, **43**, 2860 (2000).
7. M. Duflos, M. R. Nourrisson, J. Brelet, J. Courant, G. Le Baut, N. Grimaud and J. Y. Petit, *European Journal of Medicinal Chemistry*, **36**, 545 (2001).
8. M. A. S. Kumar, *Acta Pharmaceutica*, **57**, 31 (2007).
9. M. Sukuroglu, B. C. Ergun, S. Unlu, M. F. Sahin, E. Kupeli, E. Yesilada and E. Banoglu, *Archives of Pharmacol Research*, **28**, 509 (2005).
10. P. Machado, F. A. Rosa, M. Rossatto, G. S. Sant'Anna, P. D. Sauzem, R. M. S. Silva, M. A. Rubin, J. Ferreira, H. G. Bonacorso, N. Zanatta and M. A. P. Martinsa, *ARKIVOC*, **i**, 1 (2007).
11. A. Mathew, T. L. M. Sheeja, T. A. Kumar and K. Radha, *Hygeia journal for Drugs and Medicine*, **3**, 48 (2011).
12. L. Rosaria, S. Dias and R. R. S. Salvador, *Pharmaceuticals*, **5**, 317 (2012).
13. A. M. Youssef, M. S. White, E. B. Villanueva, I. M. El-Ashmawy and A. Klegeris, *Bioorganic and Medicinal Chemistry*, **18**, 2019 (2010).
14. M. Amir, H. Kumar and S. A. Javed, *Archiv der Pharmazie*, **340**, 577 (2007).
15. A. Irfan, F. Ijaz, A. G. Al-Sehemi and A. M. Asiri, *Journal of Computational Electronics*, DOI 10.1007/s10825-012-0417-8 (2012).
16. P. C. Lima, L. M. Lima, K. C. M. da Silva, P. H. O. Leda, A. L. P. de Miranda, C. A. M. Fraga and E. J. Barreiro, *European Journal of Medicinal Chemistry*, **35**, 187 (2000).
17. J. M. Figueiredo, C. A. Camara, E. G. Amarante, A. L. P. Miranda, F. M. Santos, C. R. Rodrigues, C. A. M. Fraga and E. J. Barreiro, *Bioorganic and Medicinal Chemistry*, **8**, 2243 (2000).
18. J. J. Vora, D. R. Patel, A. R. Patel and Y. S. Patel, *Asian Journal of Biochemical and Pharmaceutical Research*, **1**, 109 (2011).
19. M. J. Frisch, G. W. Trucks, H. B. Schlegel, G. E. Scuseria, M. A. Robb, J. R. Cheeseman, G. A. Scalmani, V. Barone, B. Mennucci, G. A. Petersson, H. Nakatsuji, M. Caricato, X. Li, H. P. Hratchian, A. F. Izmaylov, J. Bloino, G. Zheng, J. L. Sonnenberg, M. Hada, M. Ehara, K. Toyota, R. Fukuda, J. Hasegawa, M. Ishida, T. Nakajima, Y. Honda, O. Kitao, H. Nakai, T. Vreven, J. A. Montgomery, Jr., J. E. Peralta, F. Ogliaro, M. Bearpark, J. J. Heyd, E. Brothers, K. N. Kudin, V. N. Staroverov, R. Kobayashi, J. Normand, K. Raghavachari, A. Rendell, J. C. Burant, S. S. Iyengar, J. Tomasi, M. Cossi, N. Rega, J. M. Millam, M. Klene, J. E. Knox, J. B. Cross, V. Bakken, C. Adamo, J. Jaramillo, R. Gomperts, R. E. Stratmann, O. Yazyev, A. J. Austin, R. Cammi, C. Pomelli, J. W. Ochterski, R. L. Martin, K. Morokuma, V. G. Zakrzewski, G. A. Voth, P. Salvador, J. J. Dannenberg, S. Dapprich, A. D. Daniels, Ö. Farkas, J. B. Foresman, J. V. Ortiz, J. Cioslowski, and D. J. Fox, Gaussian 09, Revision A. 1; Gaussian, Inc.: Wallingford, CT, (2009).
20. A. Irfan and A. G. Al-Sehemi, *Journal of Saudi Chemical Society*, doi:10.1016/j.jscs.2011.11.006 (2011).
21. A. Irfan, H. Aftab and A. G. Al-Sehemi, *Journal of Saudi Chemical Society*, doi:10.1016/j.jscs.2011.11.013 (2011).
22. A. Irfan, A. G. Al-Sehemi, A. M. Asiri, M. Nadeem and K. A. Alamry, *Computational and Theoretical Chemistry*, **977**, 9 (2011).
23. A. Irfan, A. G. Al-Sehemi, S. Muhammad and J. Zhang, *Australian Journal of Chemistry*, **64**, 1587 (2011).
24. A. G. Al-Sehemi, A. Irfan, A. M. Asiri and Y. A. Ammar, *Spectrochimica Acta Part A: Molecular and Biomolecular Spectroscopy*, **91**, 239 (2012).
25. A. G. Al-Sehemi, A. Irfan, A. M. Asiri and Y. A. Ammar, *Journal of Molecular Structure*, **1019**, 130 (2012).
26. A. Irfan, N. Hina, A. G. Al-Sehemi and A. M. Asiri, *Journal of Molecular Modeling*, **18**, 4199 (2012).
27. A. Irfan, R. Cui, J. Zhang and L. Hao, *Chemical Physics*, **364**, 39 (2009).
28. A. G. Al-Sehemi, A. Irfan and A. M. Asiri, *Theoretical Chemistry Accounts*, **131**, 1199 (2012).
29. A. Irfan and A. G. Al-Sehemi, *Journal of Molecular Modeling*, **18**, 4893 (2012).

30. A. Irfan, R. Jin, A. G. Al-Sehemi and A. M. Asiri, *Spectrochimica Acta Part A: Molecular and Biomolecular Spectroscopy*, <http://dx.doi.org/10.1016/j.saa.2013.02.045> (2013).
31. A. Irfan, M. Nadeem, M. Athar, F. Kanwal and J. Zhang, *Computational and Theoretical Chemistry*, **968**, 8 (2011).
32. A. R. Chaudhry, R. Ahmed, A. Irfan, A. Shaari and A. G. Al-Sehemi, *Materials Chemistry and Physics*, <http://dx.doi.org/10.1016/j.matchemphys.2012.11.075> (2012).
33. A. Irfan, J. Zhang and Y. Chang, *Theoretical Chemistry Accounts*, **127**, 587 (2010).
34. A. Irfan, R. H. Cui and J. P. Zhang, *Theoretical Chemistry Accounts*, **122**, 275 (2009).
35. A. D. Becke, *Journal of Chemical Physics*, **98**, 5648 (1993).
36. B. Miehlich, A. Savin, H. Stoll and H. Preuss, *Chemical Physics Letters*, **157**, 200 (1989).
37. C. Lee, W. Yang and R. G. Parr, *Physical Review B*, **37**, 785 (1988).
38. J. Sun, J. Song, Y. Zhao and W. Z. Liang, *Journal of Chemical Physics*, **127**, 234107 (2007).
39. C. R. Zhang, W. Z. Liang, H. S. Chen, Y. H. Chen, Z. Q. Wei and Y. Z. Wu, *Journal of Molecular Structure (THEOCHEM)*, **862**, 98 (2008).
40. D. Matthews, P. Infelta and M. Grätzel, *Solar Energy Materials and Solar Cells*, **44**, 119 (1996).
41. N. M. O' Boyle, A.L. Tenderholt and K. M. Langner, *Journal of Computational Chemistry*, **29**, 839 (2008).